


2023

## The Numerical Study of Aeroacoustics Performance of Wings with Different Wavelength Leading-Edge Tubercles

Youjie Zhang  
*University of Central Florida*

 Part of the [Aerodynamics and Fluid Mechanics Commons](#)

Find similar works at: <https://stars.library.ucf.edu/honorsthesis>

University of Central Florida Libraries <http://library.ucf.edu>

This Open Access is brought to you for free and open access by the UCF Theses and Dissertations at STARS. It has been accepted for inclusion in Honors Undergraduate Theses by an authorized administrator of STARS. For more information, please contact [STARS@ucf.edu](mailto:STARS@ucf.edu).

---

### Recommended Citation

Zhang, Youjie, "The Numerical Study of Aeroacoustics Performance of Wings with Different Wavelength Leading-Edge Tubercles" (2023). *Honors Undergraduate Theses*. 1437.  
<https://stars.library.ucf.edu/honorsthesis/1437>

Numerical Study of Aeroacoustics Performance of Wings with Different  
Wavelength Leading-edge Tubercles

by

YOUJIE ZHANG

A thesis submitted in partial fulfillment of the requirements  
for the Honors in the Major Program in Aerospace Engineering  
in the College of Engineering and Computer Science  
and in the Burnett Honors College  
at the University of Central Florida  
Orlando, Florida

Spring Term, 2023

Thesis Chair: Michael Kinzel, Ph.D.

## **ABSTRACT**

The leading-edge tubercle is a type of airfoil modification that inspired by the humpback whale. It was found that the aerodynamic performance of the wing would increase compared to the wing without tubercles. In the past several years, a lot of numerical and experimental studies have been accomplished to explore this leading-edge modification. Besides the aerodynamic performance change, this research explores the aeroacoustics behavior of airfoils with leading-edge tubercles. A numerical study based on Computational Fluid Dynamics (CFD) is established, and simulations using Star CCM are accomplished based on reasonable set-ups. The airfoil chosen to create the wing is NACA 4412 which is an asymmetric airfoil. Two different tubercle wavelengths were used: 20 mm and 25 mm. The baseline airfoil is the wing that made of the same airfoil but without any modifications. For wings with leading-edge tubercles, the wavelength of the tubercles is the only changing parameter. It was found that the wings with leading-edge tubercles can reduce the noise generation, and the best noise reduction is achieved for a value of 2.525 dB (Decibel) at Point Receiver 10 for the wing that has 25 mm wavelength leading-edge tubercles. However, the wavelength of tubercles does not affect the aeroacoustics performance in an obvious way.

## **ACKNOWLEDGEMENTS**

I would like to express my deepest appreciation to my Thesis Chair Dr. Michael Kinzel. He gave a lot of useful suggestions during the research meetings for this research, and he always push me move forward and keep progressing. I cannot accomplish this research without his generous help. I would also like to say thank you to Dr. Ozbay and Dr. Burke for giving good advice for this project and spending valuable time for solving my questions. Finally, I appreciate to everyone who did provide help for this research and the thesis paper.

# TABLE OF CONTENTS

ABSTRACT .....	ii
ACKNOWLEDGEMENTS.....	iii
TABLE OF CONTENTS .....	iv
LIST OF FIGURES .....	v
LIST OF TABLES .....	vi
INTRODUCTION .....	1
GEOMETRY AND MODEL .....	3
COMPUTATIONAL DOMAIN STUDY .....	6
MESH STUDY .....	9
SIMULATION MODEL STUDY .....	14
AEROACOUSTIC POINT RECEIVERS .....	17
RESULTS AND DISCUSSION.....	19
LIMITATIONS .....	23
CONCLUSION.....	25
REFERENCES .....	26

## LIST OF FIGURES

Figure 1: The Wing Without Modification .....	3
Figure 2: The Wing With 20 mm Wavelength Tubercles.....	4
Figure 3: Figure 4: The Wing With 20 mm Wavelength Tubercles .....	4
Figure 5: The Inlet .....	5
Figure 6: The Outlet.....	5
Figure 7: The Baseline Computational Domain .....	6
Figure 8: Reference Value vs Domain Size .....	7
Figure 9: Number of Mesh Elements vs Cell Size.....	12
Figure 10: Number of Mesh Elements vs Cell Size.....	12
Figure 11: Number of Mesh Elements vs Cell Size.....	12
Figure 12: Final Mesh Scene for the Baseline Wing .....	13
Figure 13: Final Mesh Scene of the Wing with 20 mm Tubercles.....	13
Figure 14: Final Mesh Scene of the Wing with 25 mm Tubercles.....	13
Figure 15: Reference Value vs Turbulence Models .....	16
Figure 16: PRs Along X-Direction .....	18
Figure 17: PRs Along Spanwise-Direction .....	18
Figure 18: PRs On the Edge of the Wing.....	18
Figure 19: PR 10 SPL VS Time .....	20
Figure 20: PR 10 SPL VS Time .....	20
Figure 21: Normal Wing FH-W Pressure Contour .....	21
Figure 22: Wing with 20 mm Tubercles FH-W Pressure Contour.....	21
Figure 23: Wing with 20 mm Tubercles FH-W Pressure Contour.....	22

## LIST OF TABLES

Table 1: The Computational Domain Size Study.....	7
Table 2: Mesh Study of the Wing Without Tubercles .....	10
Table 3: Mesh Study of the Wing With 20 mm Tubercles .....	10
Table 4: Mesh Study of the Wing With 25 mm Tubercles .....	11
Table 5: Results of Simulations Under Varied Models .....	16

## INTRODUCTION

Aeroacoustics is a field that belongs to acoustic but is specifically applied in aerospace engineering that focuses on the noise generation by turbulent fluid motion that due to unsteady fluid fluctuations, or aerodynamic forces that interact with surfaces such as lift and drag [1]. The study of aeroacoustics is significant and essential, not only because it can help engineers to reduce harmful noise to make passengers have a more comfortable environment during the flight, but also decrease harmful vibrations and structural fatigue [2]. The first person who related sound generation to fluid motion was probably Strouhal. After his experimental investigation of Aeolian tones generated by a stretched wire, he stated that the fluid friction was the reason. Even though the conclusion is incorrect, that was a milestone of exploring the relationship between noise and fluid motion. In 1915, Lord Rayleigh related the radiation to the periodic vortex shedding, and that was the first moment that aeroacoustics became a branch of flow physics. The giant step of experimental aeroacoustics came from the evidence of the extreme acoustic nuisance caused by the first jet engines that was brought by the pioneer, Sir J. Lighthill [3]. This field of study could be divided into two branches which are experimental aeroacoustics and computational aeroacoustics, and they are also the methods to explore the aeroacoustics performance of an object. This paper will focus on the Computational Aeroacoustics (CAA). CAA is an approach that uses numerical techniques and the power of computers to study the noise generation in Aerospace Engineering. Since all the aeroacoustics mechanisms such as source generation, acoustic propagation, refraction, and scattering are related to fluid dynamics,



it is achievable to perform simulations by using the Navier-Stokes equations from the source region to the far field [4]. This method also motivated a new type of aeroacoustics experiment which is called benchmark experiments that provide verifications, validation, and calibration data for CFD [2]. Both numerical and experimental studies are helpful for aeroacoustics analysis, and scientists have made a lot of effort and progress to apply their findings in the aerospace field, such as leading-edge noise reduction. The leading-edge noise, also called the turbulence-impingement noise, is generated by aerodynamic interaction between a solid body and a turbulent inflow. Some techniques have been proposed to reduce the leading-edge noise. The leading-edge tubercle is one of the examples. It is a wing modification that is inspired by the humpback whale. It was found that the leading-edge tubercles are not only able to improve the aerodynamics performance at stall conditions, but also can reduce the noise from leading edge of the wing [5].

It can be expected that passengers could be more enjoyable during the flight because of the reduced noise from the aircraft. The Aeroacoustics is the subject that can help to make this come true.

## GEOMETRY AND MODEL

All the wing models are three dimensional (3D), and the airfoil for the wing is NACA 4412. The main reason to choose this airfoil is that previous research already studied the aeroacoustics performance of wings that made of symmetric airfoil such as NACA 0021, so it is necessary to extend the research on wings that made of asymmetric airfoil. The chord length of the wing is 100 millimeter (mm), and spanwise direction length is also 100 mm for all wing geometries. The AOA (angle of attack) is 0 degrees for all wing models.



Figure 1: The Wing Without Modification

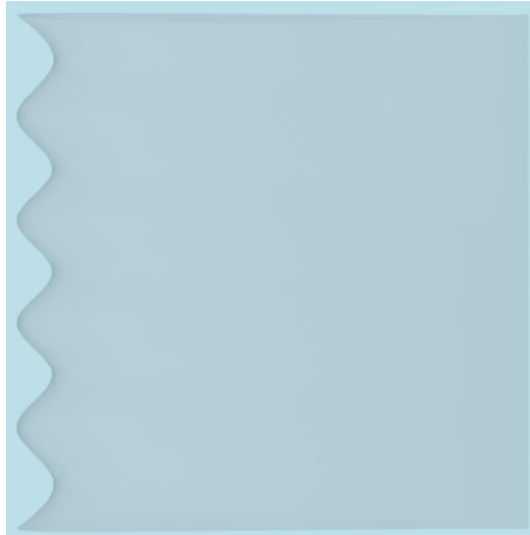


Figure 2: The Wing With 20 mm Wavelength Tubercles

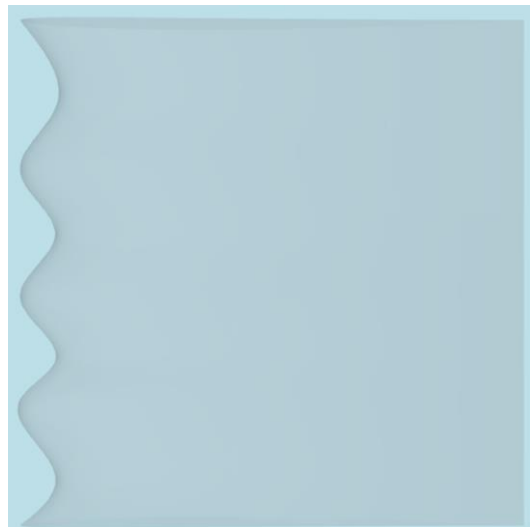


Figure 3: Figure 4: The Wing With 20 mm Wavelength Tubercles

Above pictures (Figure 1 to Figure 3) show the geometry and domain set up. The distance from the block inlet to the leading edge of the wing is 200 mm, and the distance from the trailing edge to the block outlet is 100 mm. The distance from the top side of the block to the wing and the bottom side to the wing are the same which is 100 mm. The Subtract operation is used to create the proper domain that Star CCM can operate with. The target body is the block, and the tool body is the wing. In the simulation, the air flow would enter the inlet and exit via the outlet,

so the direction of the air flow is the positive x-direction. For other faces of the block are boundaries, there would not be any air flow. The inlet is velocity inlet with 0 velocity as initial condition and then accelerated to 40 m/s, and the outlet is pressure outlet with zero pascal pressure. Other faces of the domain are labeled as symmetry plane. The wing is the Wall type which would be the focus of the study in the domain.

Simcenter STAR-CCM+

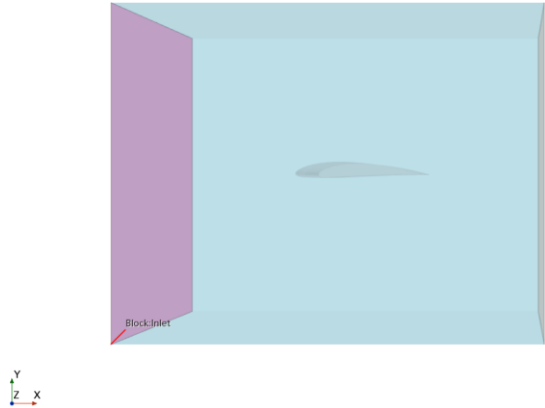


Figure 5: The Inlet

Simcenter STAR-CCM+

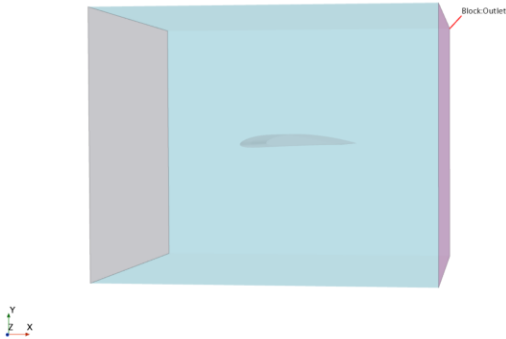


Figure 6: The Outlet

## COMPUTATIONAL DOMAIN STUDY

It is indispensable and beneficial to study the size of computational domain in CFD because it is a key factor that can influence the accuracy of simulation results and the computational expense [6]. The baseline size of the computational domain size is the one that from similar research done by Fan Tong *et al* [7]. However, the rod-airfoil interaction will not be studied so the computational domain for this research only includes the wing. The computational domain size is based on the percentage of the baseline domain size from 10% to 50%. For example, 10% of the baseline domain size means the distance from inlet to the leading-edge is  $1.3c$  (1.3 times the chord length), the distance from leading-edge to the outlet is  $2.0c$ , and the height of the computational domain is  $2.6c$ . The reference value to monitor the domain size influence is the Sound Pressure Level (SPL) in Pascals of Point Receiver (PR) 12 at the last time step of the simulation. To optimize the time for each complete simulation, the Mesh Base Size of the domain is also increasing with the increasing percentage of the baseline domain size.

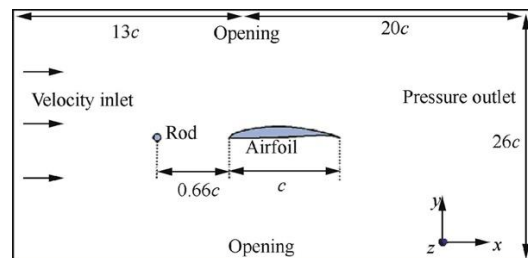


Figure 7: The Baseline Computational Domain

Table 1: The Computational Domain Size Study

Percentage of the Baseline Domain Size	X-Direction Length of the Domain	Y-Direction Length of the Domain	Mesh Base Size (mm)	PR 12 SPL at $t=0.99s$ (Pa)	Result Error (%)
10%	X1: 1.3c X2: 2c	2.6c	5	4.81758	0
20%	X1: 2.6c X2: 4c	5.2c	10	4.80043	0.356
30%	X1: 3.9c X2: 6c	7.8c	15	4.75597	0.926
40%	X1: 5.2c X2: 8c	10.4c	20	4.69883	1.201
50%	X1: 6.5c X2: 10c	13c	25	4.70627	0.158

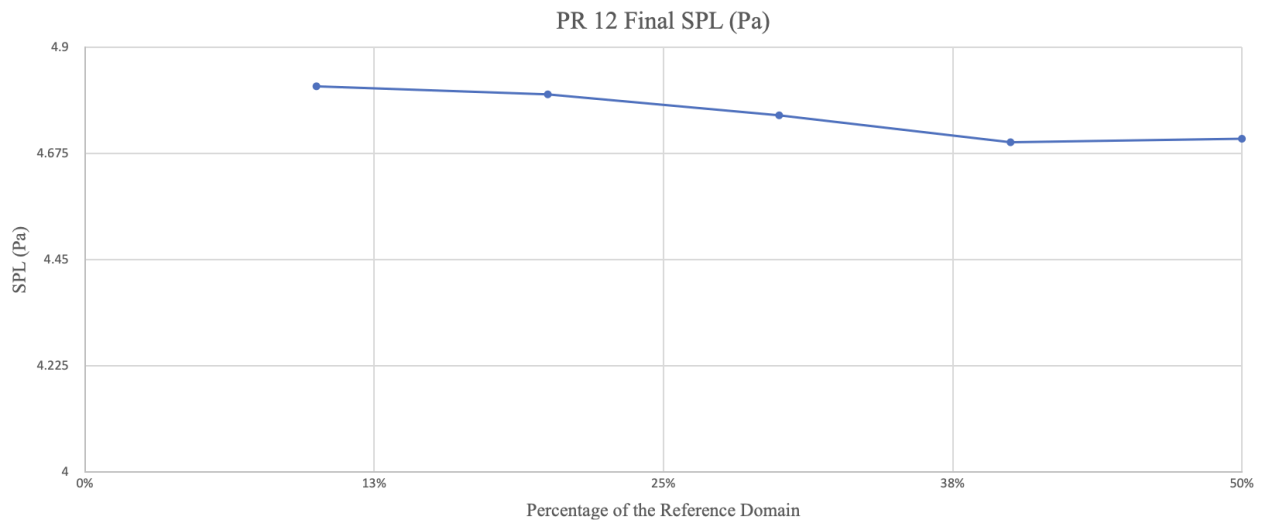


Figure 8: Reference Value vs Domain Size

The table and plot above show the results for the computational domain size study. X1 is the distance from leading-edge of the wing to the inlet, and X2 is the distance from the leading-

edge of the wing to the outlet. The maximum change in reference value is 1.201% and the minimum change in reference is 0.158%. With these negligible changes in reference value, it can be concluded that the size of the computational domain does not have significant influence on this research. Therefore, the 10% of the baseline domain size is used for the simulation to save computational performance and time.

## MESH STUDY

Due to the complexity of the overall geometry, using meshing allows the computer to discretize the object into small cells and solve the governing partial differential equations in these small cells and then provide the solution for the comprehensive simulation [8]. Thus, the quality of mesh can significantly influence the results, convergence, and the time needed to finish the simulation. To obtain as accurate results as possible and minimize the simulation time, it is extremely necessary to do the mesh study for the object to optimize the quality of mesh. For this research, the focus of the study is the wing. Therefore, the mesh quality of the wing surface should be the most concerning part. The Mesh Base Size for the Block is 5 mm since the 10% of the baseline domain size is used and it is not the concentration. Three mesh models are adopted for all the simulations: Prism Layer Mesher, Surface Remesher, and Trimmer. The surface growth rate, default growth rate, and boundary growth rate are chosen to be slow in order to have better quality of mesh near boundaries. The volumetric control is used for the wing so the mesh quality of the wing could be controlled individually. The goal of mesh study is to obtain the results that are independent of mesh. For achieving the goal, the relationship between mesh size and reference value fluctuations must be explored. The cell sizes chosen are 1.75 mm, 1.5 mm, 1.25mm, 1.0 mm, 0.75 mm, and 0.5 mm, and the reference value is the SPL of PR 12 at the last time step. The cell size is the only changing parameter, other mesh conditions and values are identical along all simulations and wing models.



The tables and plots below show the detailed information of mesh study for the wing without tubercles, the wing with 20 mm wavelength tubercles, and the wing with 25 mm wavelength tubercles.

Table 2: Mesh Study of the Wing Without Tubercles

Element Size (mm)	Number of Cells	Number of Faces	Number of Vertices	PR 12 SPL at $t=0.99s$ (Pa)	Change in Results (%)
1.75	551117	1667527	595894	5.24729	0
1.5	551314	1662524	590507	5.38836	2.688
1.25	589666	1781486	633710	5.18259	3.819
1	1583358	4790459	1689208	4.89739	5.503
0.75	1762443	5317752	1863406	4.88356	0.282
0.5	2329963	7031281	2458533	4.80810	1.545

Table 3: Mesh Study of the Wing With 20 mm Tubercles

Element Size (mm)	Number of Cells	Number of Faces	Number of Vertices	PR 12 SPL at $t=0.99s$ (Pa)	Change in Results (%)
1.75	582125	1752577	618932	Diverged	0
1.5	588912	1774871	627267	4.34703	0

1.25	602179	1814579	641265	4.40221	1.269
1	1758489	5294366	1845660	4.10448	6.763
0.75	1984949	5955388	2060127	4.05382	1.234
0.5	2791626	8366191	2878743	3.99045	1.563

Table 4: Mesh Study of the Wing With 25 mm Tubercles

Element Size (mm)	Number of Cells	Number of Faces	Number of Vertices	PR 12 SPL at $t=0.99s$ (Pa)	Change in Results (%)
1.5	571205	1723484	611540	Diverged	0
1.25	583425	1760362	624005	Diverged	0
1 mm	596494	1799599	637373	4.40019	0
0.75	1716696	5174417	1808721	4.10647	6.675
0.5	1957759	5881559	2040130	4.08792	0.452

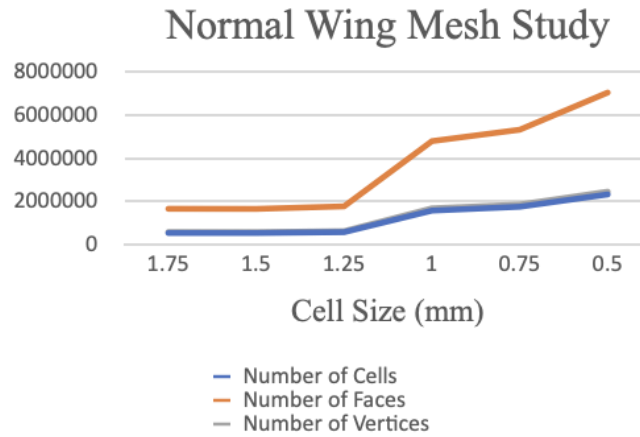


Figure 9: Number of Mesh Elements vs Cell Size

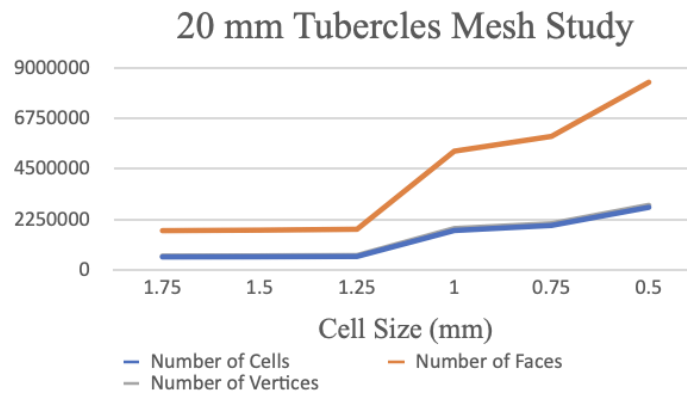


Figure 10: Number of Mesh Elements vs Cell Size

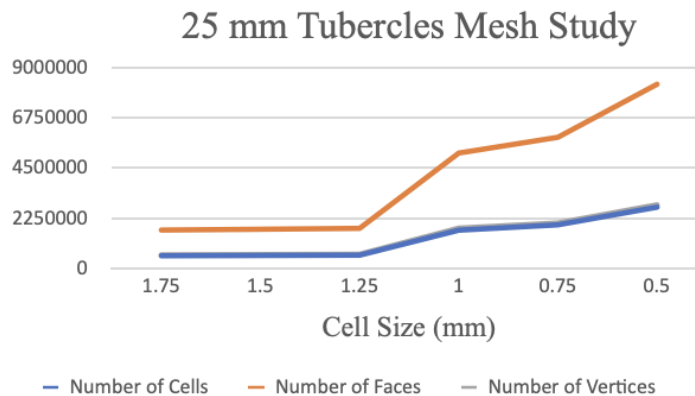


Figure 11: Number of Mesh Elements vs Cell Size

The Number of Cells, Number of Faces, and Number of Vertices are drastically increased when the Mesh Cell Size is reduced to 1 mm. Also, the fluctuation of the reference value can be ignored. Another conclusion can be made depending on the results is that the wings with leading-

edge tubercles require smaller Mesh Cell Size to have convergent simulation results. It might be because the inherent complicated geometry of the tubercles. All the final simulations for the wing models are using 1 mm Mesh Cell Size to balance the simulation time and the result accuracy. In fact, the Mesh Study can be pushed further and more representative by changing other parameters and using different mesh models to obtain the supreme quality of mesh.



Figure 12: Final Mesh Scene for the Baseline Wing

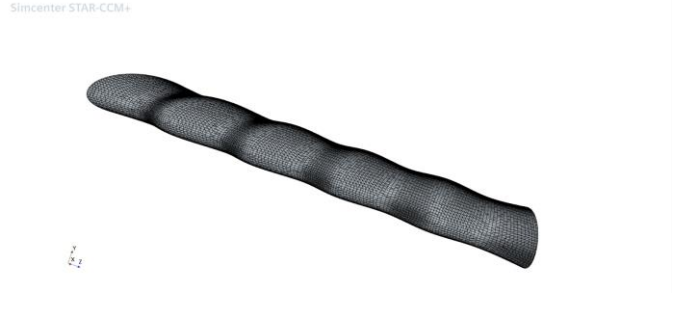


Figure 13: Final Mesh Scene of the Wing with 20 mm Tubercles

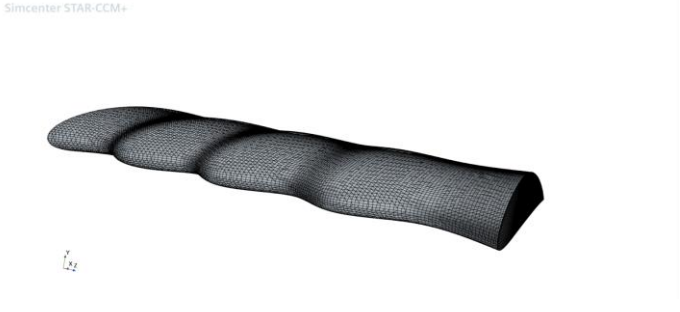


Figure 14: Final Mesh Scene of the Wing with 25 mm Tubercles

## SIMULATION MODEL STUDY

The Star CCM provides many options for adapting different simulations with various purposes, such as flow type, wall treatment methods, and turbulence models. etc. It is impossible to state that there is a combination of simulation settings will be suitable for all the simulations with all the conditions because the selection of these settings must be based on the specific project. For example, simulating a supersonic Converging-Diverging Nozzle requires nonidentical settings than simulating a wing under low Mach Number flow because the properties of the air would be changed, and the fluid flow regimes are different. Therefore, having clear understanding of the project is highly essential for selecting proper simulation models in order to obtain useful and accurate results.

Based on previous research, the Large Eddy Simulation (LES) with Smagorinsky Subgrid Scale is commonly used for predicting the aeroacoustics performance of a 3D wing [7] [9]. However, to study how the turbulence models influence the results, five models are used for the simulations, they are LES (Model A0, Detached Eddy Simulation (Model B), K-epsilon (Model C), K-omega (Model D), and Laminar (Model E). The inlet velocity is 40 m/s, and the calculated Reynolds Number is 254,976. Compared to the magnitude of chord length and spanwise-direction length of the wing, the thickness of it can be negligible. Then it will be reasonable to apply the Thin Plate Theory, so the critical Reynolds Number is 500,000 which means the flow over the object will become turbulent from laminar if the Reynolds Number exceeds this value. The fluid used for the simulation is air with constant density and dynamic viscosity which is

1.1825 kg/m<sup>3</sup> and 1.85508E-5 Pa respectively. Since the inlet velocity is low which is less than 1.0 Mach number, Segregated flow solver was chosen because it requires less memory and most importantly, the inlet velocity is subsonic. Coupled flow solver is widely used for supersonic flows and objects where the shock waves are produced due to large pressure gradients. Implicit Unsteady model was utilized with 0.01s timestep, and second order temporal discretization was selected to obtain more accurate results [10].

Equation 1 through 4 show the 3D unsteady form of Navier-Stokes Equations, and they are the important parameters to determine the convergence of the results.

$$\text{Continuity: } \frac{\partial \rho}{\partial t} + \frac{\partial(\rho u)}{\partial x} + \frac{\partial(\rho v)}{\partial y} + \frac{\partial(\rho w)}{\partial z} = 0 \quad (1)$$

$$X - \text{Momentum: } \frac{\partial(\rho u)}{\partial t} + \frac{\partial(\rho u^2)}{\partial x} + \frac{\partial(\rho uv)}{\partial y} + \frac{\partial(\rho uw)}{\partial z} = -\frac{\partial p}{\partial x} + \frac{1}{Re} \left\{ \frac{\partial \tau_{xx}}{\partial x} + \frac{\partial \tau_{xy}}{\partial y} + \frac{\partial \tau_{xz}}{\partial z} \right\} \quad (2)$$

$$Y - \text{Momentum: } \frac{\partial(\rho v)}{\partial t} + \frac{\partial(\rho uv)}{\partial x} + \frac{\partial(\rho v^2)}{\partial y} + \frac{\partial(\rho vw)}{\partial z} = -\frac{\partial p}{\partial y} + \frac{1}{Re} \left\{ \frac{\partial \tau_{xy}}{\partial x} + \frac{\partial \tau_{yy}}{\partial y} + \frac{\partial \tau_{yz}}{\partial z} \right\} \quad (3)$$

$$Z - \text{Momentum: } \frac{\partial(\rho w)}{\partial t} + \frac{\partial(\rho uw)}{\partial x} + \frac{\partial(\rho vw)}{\partial y} + \frac{\partial(\rho w^2)}{\partial z} = -\frac{\partial p}{\partial z} + \frac{1}{Re} \left\{ \frac{\partial \tau_{xz}}{\partial x} + \frac{\partial \tau_{yz}}{\partial y} + \frac{\partial \tau_{zz}}{\partial z} \right\} \quad (4)$$

The main reason for not using Steady model is that the Ffowcs Williams-Hawkings (FW-H) aeroacoustics model only can be used under unsteady condition. FW-H is a methodology that can perform Far-field sound propagation. If the Mach number is low, it can be assumed that the volume sources are much weaker than the surface sources and can be neglected. Then, as the equation 1 shows, the integral equation can be obtained for far-field acoustic pressure at a specific location and time step in the simulation domain [11].

$$p'(x, t) = \frac{1}{4\pi|1-M_r|_x} \left( \frac{\partial}{\partial t} \iint [\rho_0 u_i n_i + \rho'(u_i - U_i) n_i] d\Sigma + \frac{x_i}{c|x|} \frac{\partial}{\partial t} \iint [p'^{n_i} + \rho u_i (u_j - U_j) n_j] d\Sigma \right) \quad (5)$$

Table 5: Results of Simulations Under Varied Models

Model A	Reference Value (Pa): 4.61050
Model B	Reference Value (Pa): 4.65794
Model C	Reference Value (Pa): 4.80169
Model D	Reference Value (Pa): 4.90548
Model E	Reference Value (Pa): 4.89739

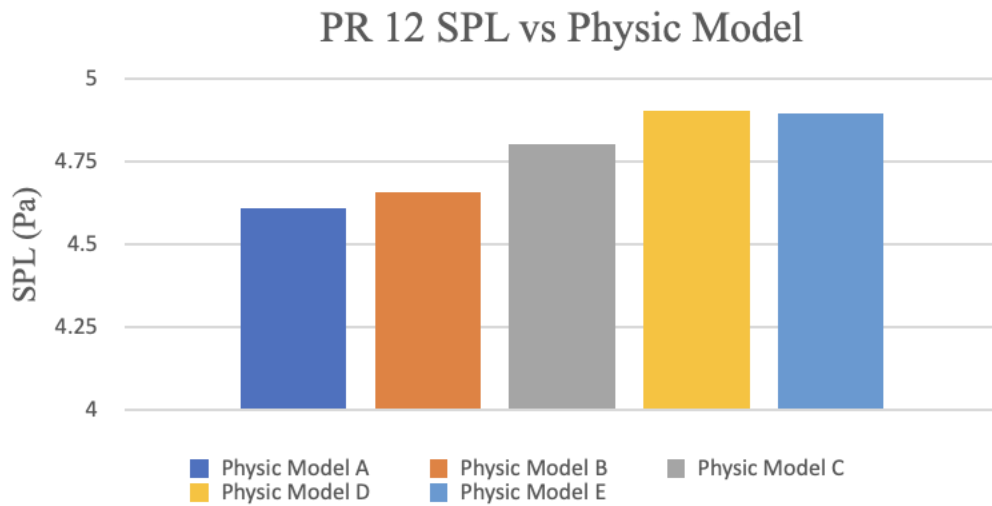


Figure 15: Reference Value vs Turbulence Models

Surprisingly the reference value does not vary obviously as the turbulence models change. It indicates that the simulation results will not be sensitive to the models. The reason behind it is still unknown due to the limited knowledge to CFD and turbulence models, however, it is a favorable phenomenon because the model that takes least time and computational performance can be selected without affecting the results notably. Hence, the Laminar model is selected for all the final simulations depending on the turbulence model study and the Reynolds Number.

## **AEROACOUSTIC POINT RECEIVERS**

The FW-H model allows the user to put far-field Point Receivers (PRs) in the interested domain and collect acoustic data. This research project includes twelve PRs for each wing model, and the positions of these PRs are determined after consideration. As figure 16 shows, there are five PRs in the middle and front of the wing (along the X-direction). PR 1 is the closest one to the wing and PR 14 is the furthest. Two reasons to put these five PRs: 1. To study the aeroacoustics performance in front of the wing. 2. To verify simulation results by analyzing the relationship between SPL and the distance from the wing. The SPL values should be decreased as the increased distance from the wing which is the noise resource. There are also five PRs along the spanwise-direction (along the Z-direction) to study how the tubercles influence the noise generation. PR 9, 10, 11, 12 are the PRs that near the edge of the wing surface to analyze the noise generation in this area. No PR is put behind the wing model because it is not the interested area of study. The Figure 14 through 16 show the locations of all PRs in the computational domain. The data from these PRs will be extracted to Excel to make plots and perform essential calculations for the Results and Discussion section.



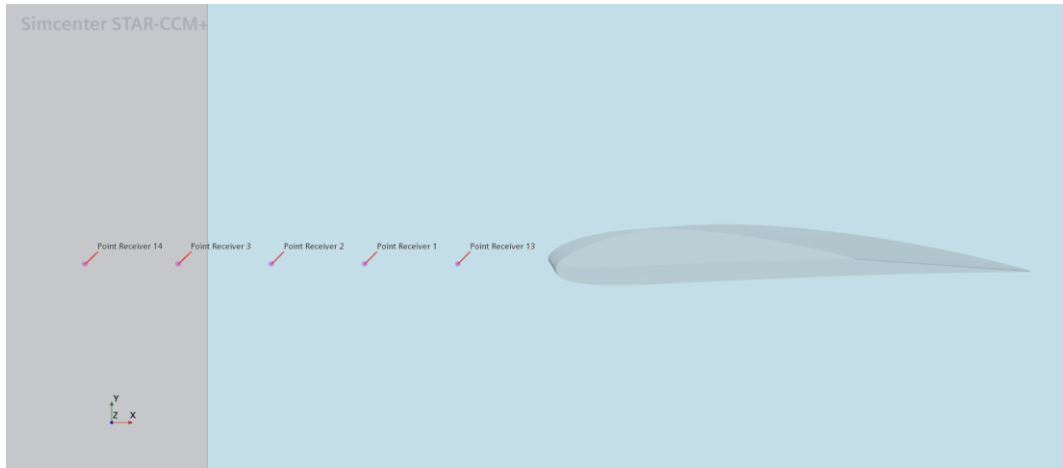


Figure 16: PRs Along X-Direction

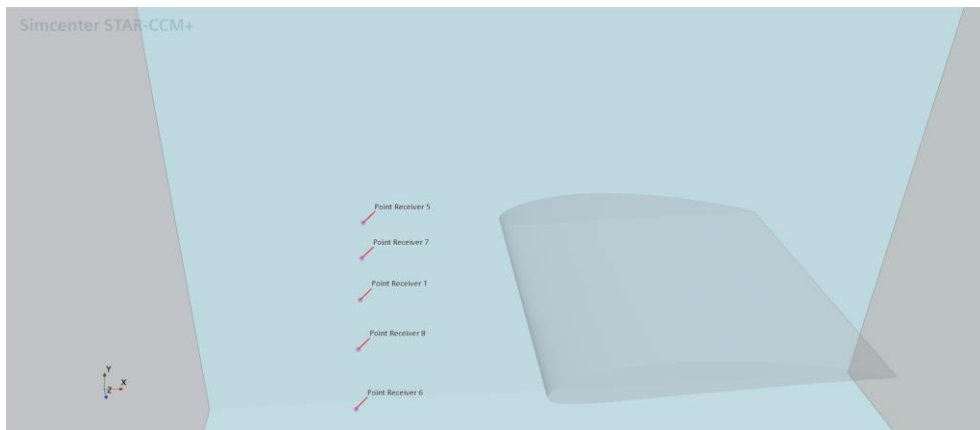


Figure 17: PRs Along Spanwise-Direction

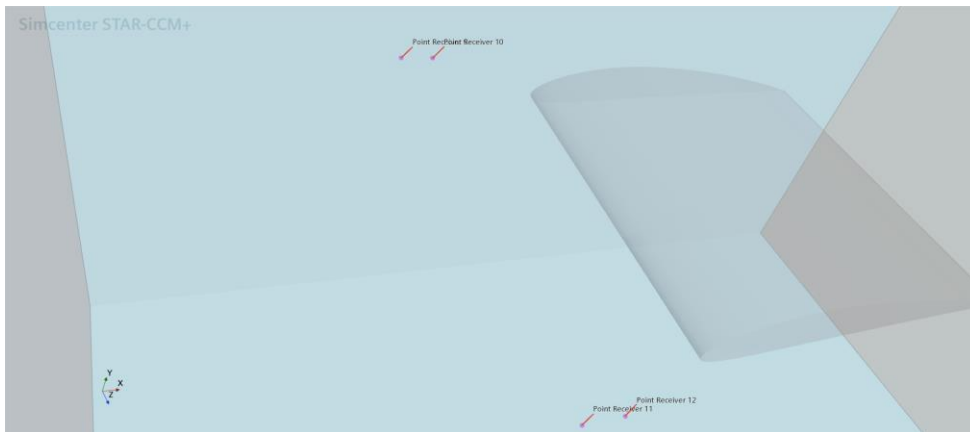


Figure 18: PRs On the Edge of the Wing

## RESULTS AND DISCUSSION

The wing models with leading-edge tubercles have lower noise generation compared to the wing without any modifications for every PR, and it can be stated that the tubercles are useful for noise reduction of a wing. The levels of noise reduction are different because of the locations of the PRs. The average noise reduction for the PRs along the X-direction is 0.303 dB for the wing with 20 mm wavelength tubercles and this value is increased to 0.369 dB for the wing with 25 mm wavelength tubercles. The value of average noise reduction for the PRs along the Z-direction is 0.361 dB for the wing with 20 mm wavelength tubercles, and 0.432 dB for the wing with 25 mm wavelength tubercles. The noise reduction near to the edge of the wing models are better. For PR 9 and 11, the average noise reduction is 1.341 dB and 0.917 dB respectively for the wing with 20 mm wavelength tubercles. At these locations, the wing model with 25 mm wavelength tubercles have close noise reduction: 1.386 dB and 0.993 dB. For PR 10 and PR 12, the average values of noise reduction are the highest: 2.481 dB and 1.534 dB for the wing with 20 mm wavelength tubercles; 2.525 dB and 1.533 dB for the wing with 25 mm wavelength tubercles. However, the difference of average noise reduction values between 20 mm wavelength tubercles and 25 mm wavelength are small or even negligible. The plots below show the best two locations for noise reduction.

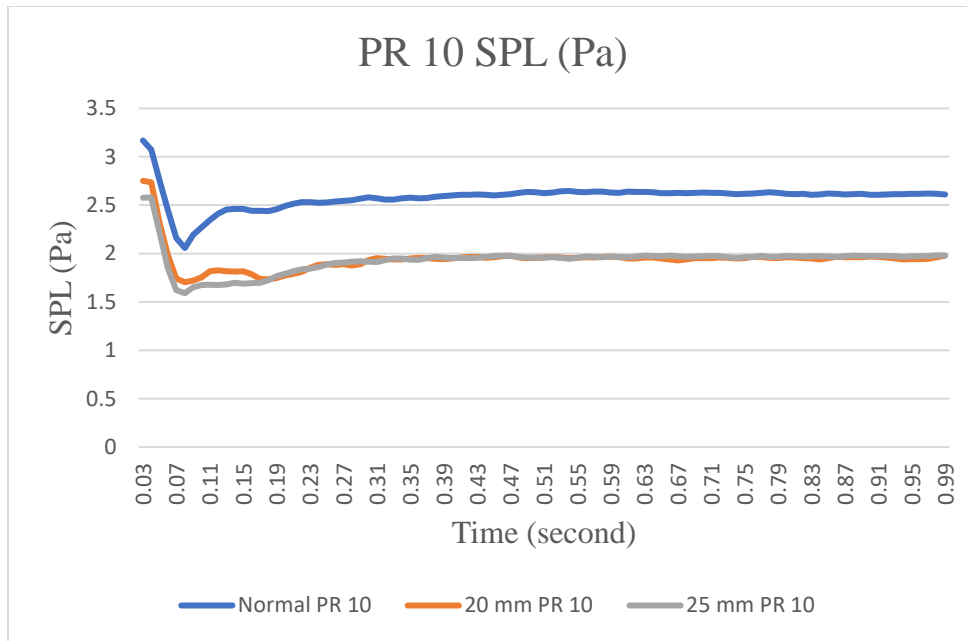


Figure 19: PR 10 SPL VS Time

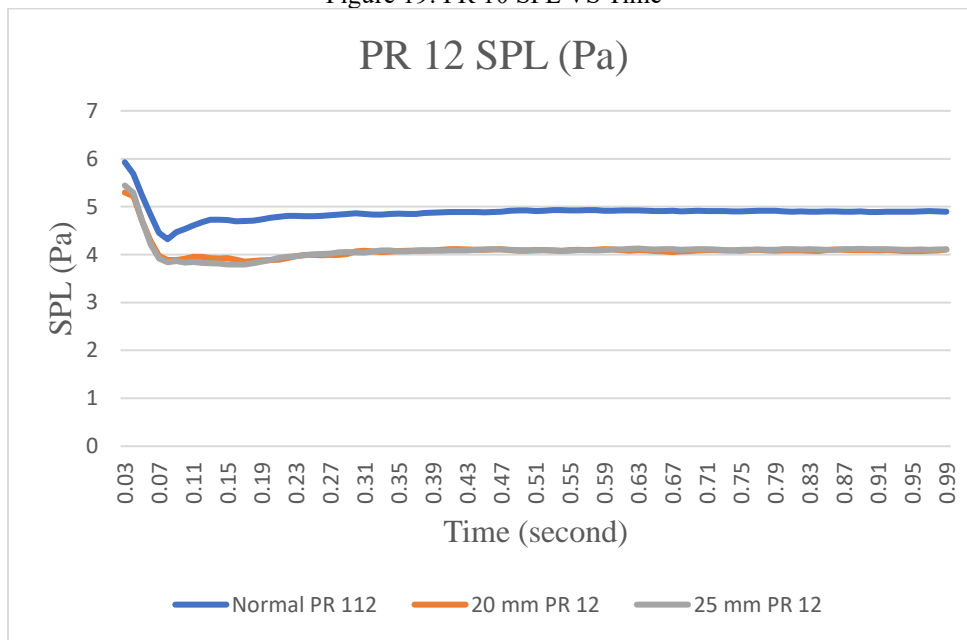


Figure 20: PR 10 SPL VS Time

The concept behind the noise reduction is the decreased pressure fluctuations. The figures below are the FW-H pressure contours to show the magnitudes of pressure fluctuations for the

wing models.

Simcenter STAR-CCM+

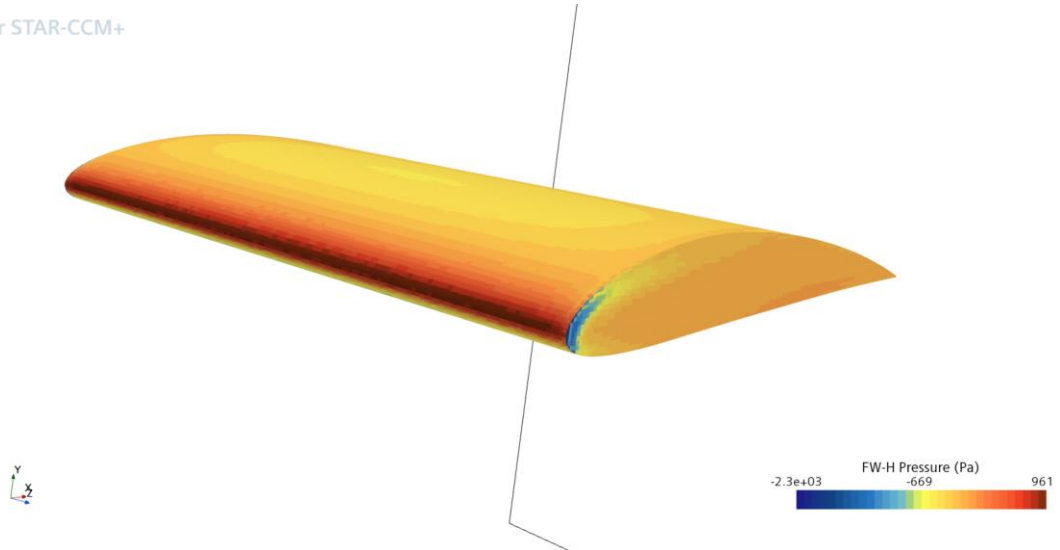


Figure 21: Normal Wing FH-W Pressure Contour

Simcenter STAR-CCM+

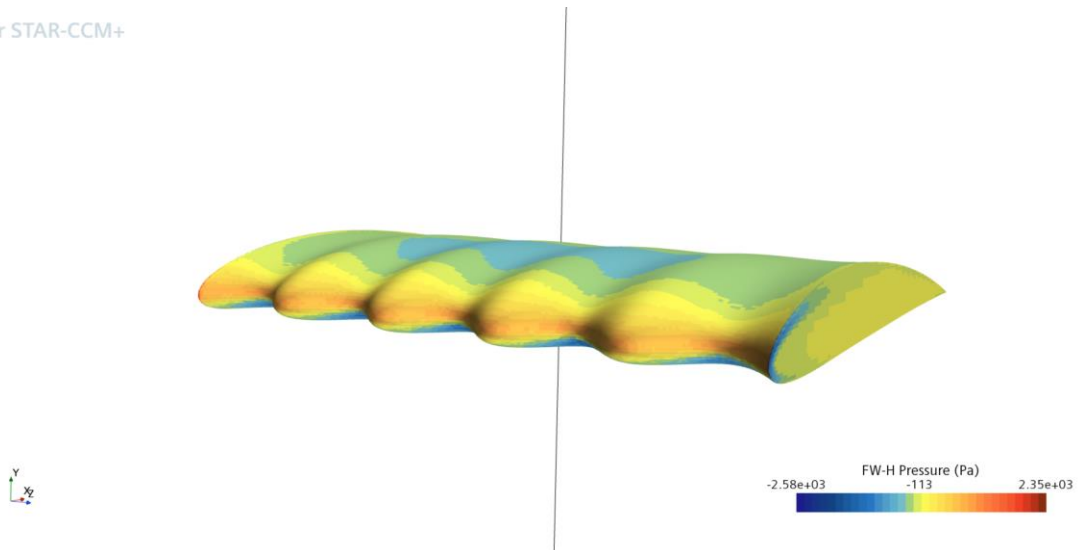


Figure 22: Wing with 20 mm Tubercles FH-W Pressure Contour

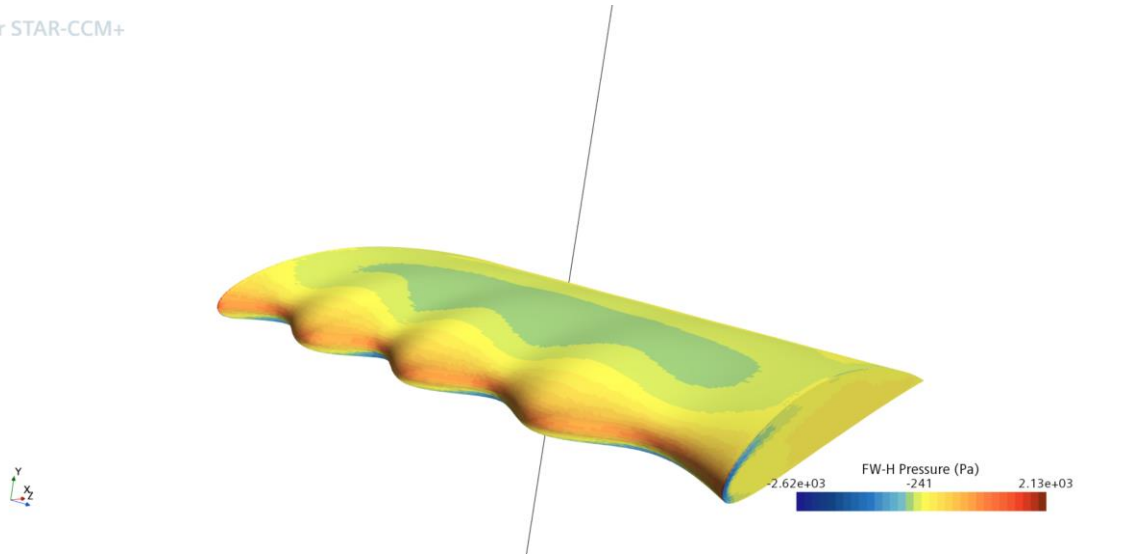


Figure 23: Wing with 20 mm Tubercles FH-W Pressure Contour

It can be seen that the wing models with leading-edge tubercles have lower FW-H Pressure which means the pressure fluctuations are less than the wing without tubercles. However, the reason why the pressure fluctuations could be reduced with tubercles is still unknown.

## LIMITATIONS

The first limitation of this research is the fact that only two different wavelength leading-edge tubercles are used. One of the conclusions from this research is that the noise reduction is not sensitive to the wavelength of tubercles. This conclusion can be more reliable and persuasive if there are more models with more varied wavelength of tubercles are included. The second limitation comes from the Turbulence Model Study. Even though the conclusion is that the turbulence mode does not affect the simulation results a lot, it cannot be ignored that most of the previous research used Large Eddy Simulation for the similar numerical study because Large Eddy Simulation has been verified by the experimental tests. By using the Laminar Model, the data of the turbulent intensity of the models cannot be obtained and this parameter could influence the noise generation because the interaction between turbulent flow and the wing can be one of the noise resources of the wing. The third limitation is that this paper does not provide the detailed explanation of the noise reduction mechanism of leading-edge tubercles. As mentioned in the Results and Discussion section, the leading-edge tubercles can reduce the pressure fluctuations and then the magnitude of the noise level will be reduced. However, it cannot be verified that it is the only reason for the noise reduction. The behavior of the flow inside the computational domain, near to the wing surface, and close to the boundaries should be analyzed and studied to find other potential reasons for the noise reduction. Finally, the study of noise frequency is missing. SPL is not the sole parameter to study the characteristics of the noise. The

frequency of the noise is the number of pressure variations per second [12]. It is also an important factor to classify different types of noise.

## CONCLUSION

This research is supposed to explore the noise performance of wings with different wavelength leading-edge tubercles, and the overall results imply that this kind of wing modification can reduce the noise level of the leading edge due to the decreased pressure fluctuations. The numerical study includes Computational Domain Study, Mesh Study, and Simulation Model Study. The final settings for the simulations are based on the results from these studies. Deeper research can be extended in the future to compare the simulation results with the experimental results; thus, the most proper and accurate simulation model can be determined to produce more realistic results. Some limitations of the research that mentioned above can also be avoided to make the study more reliable. This this research is helpful for researchers who are new to Computational Aeroacoustics and noise analysis, and it provides ideas to extend the study into a higher level of expertise. The experimental test will also be necessary to be performed to further verify and prove the theory.

,



## REFERENCES

- [1] X. Sun and X. Wang, *Fundamentals of aeroacoustics with applications to Aeropropulsion Systems*. London: Elsevier ; AP Academic Press, 2021.
- [2] “Aeroacoustics – Jet Noise,” *Theoretical fluid dynamics and Turbulence Group*. [Online]. Available: <https://faculty.eng.ufl.edu/fluids/research/aeroacoustics/#:~:text=Aeroacoustics%20%E2%80%93%20Jet%20Noise&text=Aeroacoustics%20is%20an%20important%20subject,limit%20to%20rockets%20and%20aircraft>. [Accessed: 28-Mar-2023].
- [3] Jacob, Marc C. Introduction to experimental aeroacoustics, Lecture 1. ( In Press: 2017) In: *Design and Operation of Aeroacoustic Wind Tunnels for Ground and Air Vehicles*. Von Karman Institute, Brussels, Belgium, 1-26
- [4] E. Manoha, S. Redonnet, and S. Caro, “Computational aeroacoustics,” *Encyclopedia of Aerospace Engineering*, pp. 1–16, 2010.
- [5] C. Teruna, F. Avallone, D. Casalino, and D. Ragni, “Numerical Investigation of Leading Edge noise reduction on a rod-airfoil configuration using porous materials and Serrations,” *Journal of Sound and Vibration*, vol. 494, p. 115880, 2021.
- [6] Y. Abu-Zidan, P. Mendis, and T. Gunawardena, “Optimising the computational domain size in CFD simulations of Tall Buildings,” *Heliyon*, vol. 7, no. 4, 2021.
- [7] F. TONG, W. QIAO, W. CHEN, H. CHENG, R. WEI, and X. WANG, “Numerical Analysis of broadband noise reduction with Wavy Leading Edge,” *Chinese Journal of Aeronautics*, vol. 31, no. 7, pp. 1489–1505, 2018.
- [8] Author Cadence CFD, “The importance of meshing in CFD and structural FEA,” *Cadence*, 13-Oct-2022. [Online]. Available: <https://resources.system-analysis.cadence.com/blog/msa2022-the-importance-of-meshing-in-cfd-and-structural-fea>. [Accessed: 19-Apr-2023].
- [9] W. Chen, L. Zhang, L. Wang, Z. Wei, and W. Qiao, “Utilization of whale-inspired leading-edge tubercles for airfoil noise reduction,” *Journal of Bionic Engineering*, vol. 19, no. 5, pp. 1405–1421, 2022.

- [10] A. Alonzo-García, C. del Gutiérrez-Torres, and J. A. Jiménez-Bernal, “Computational fluid dynamics in turbulent flow applications,” *Numerical Simulation - From Brain Imaging to Turbulent Flows*, 2016.
- [11] A. Bodling and A. Sharma, “Numerical investigation of noise reduction mechanisms in a bio-inspired airfoil,” *Journal of Sound and Vibration*, vol. 453, pp. 314–327, 2019.
- [12] “Characteristics of sound and the decibel scale,” *Sound and Noise - Characteristics of Sound and the Decibel Scale*. [Online]. Available: [https://www.epd.gov.hk/epd/noise\\_education/web/ENG\\_EPD\\_HTML/m1/intro\\_5.html#:~:text=The%20number%20of%20pressure%20variations,pitched%20a%20sound%20is%20perceived.](https://www.epd.gov.hk/epd/noise_education/web/ENG_EPD_HTML/m1/intro_5.html#:~:text=The%20number%20of%20pressure%20variations,pitched%20a%20sound%20is%20perceived.) [Accessed: 21-Apr-2023].